Exploring the limits of a hybrid actuation system through Co-Design

Gianluigi Grandesso, Gabriel Bravo-Palacios, Patrick Wensing, Marco Fontana, Andrea del Prete

Exploring the limits of a hybrid actuation system through Co-Design

Gianluigi Grandesso[1], Gabriel Bravo-Palacios[2], Patrick M. Wensing[3], Marco Fontana[4], Andrea Del Prete[5]

***Abstract*— This letter assesses the energy efficiency of a hybrid actuation architecture combining Geared Motors (GMs) and Series Elastic Actuators (SEAs) by comparing its energy consumption to GM and SEA alone. We consider this comparison for two robotic systems performing different tasks. Our results show that using the hybrid actuation we can save up to 98% of energy with respect to SEA for sinusoidal movements. This efficiency is achieved by exploiting the coupled dynamics of the two actuators, resulting in a latching-like control strategy. We also show that these large energy savings are not straightforwardly extendable to nonsinusoidal movements, but smaller savings (*e.g.*, 7%) are nonetheless possible. The presented results were obtained thanks to the framework of concurrent design (co-design), namely the simultaneous optimization of hardware parameters and control trajectories. This shows that the combination of complex hardware morphologies and advanced numerical co-design can lead to peak hardware performance that would be unattainable by human intuition alone.**

I. Introduction

In the last decades, many roboticists focused their research on determining which actuation mechanisms are most suitable for robotic systems such as legged robots or industrial manipulators [1]–[5]. Often, the "stiffer is better" rule of thumb has been adopted as a premise of the design process. High bandwidth force control and accurate position control were the two main benefits, however to the detriment of safety in human-machine interactions and high cost of the mechanical system. While active control is able to regulate output impedance, there are fundamental limits to mechanical robustness in the case of impulsive loads. Thus, many have taken inspiration from nature, intentionally including compliance in actuation systems between the load and mechanical energy source.

To date, there is no actuation mechanism that uniformly outperforms the others. This is due to the strong dependency on the task (*e.g.*, walking, holding objects, pick-and-place operations) that the system has to perform, and on the environment (*e.g.*, structured, unknown, with humans) in which it operates. Moreover, relative performance depends heavily on the performance index (*e.g.*, energy consumption, task completion time, accuracy) that is considered. Thus, in the robot design process, a large variety of factors have to be weighed and designers inevitably have to deal with many trade-offs.

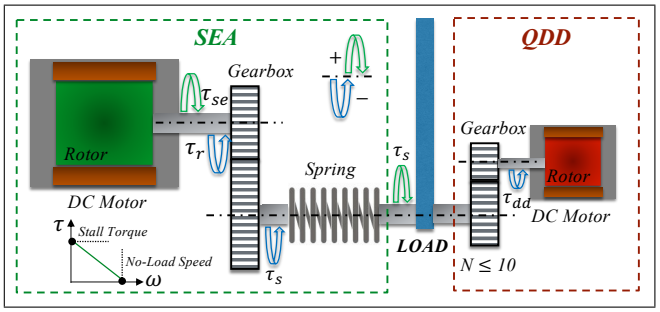

Fig. 1. Schematic of the hybrid actuation system: an SEA and a QDD work in parallel to actuate a single revolute joint.

Among those actuation mechanisms that use DC motors, the two that are most often employed are Series Elastic Actuation (SEA) [6] and Quasi-Direct Drive (QDD) motors [7] (*i.e.*, low-gear ratio actuators). In an SEA, the motor is connected to a gearbox, which in turn is attached to one end of a spring, with the other end of the spring attached to the joint output. In terms of benefits, SEAs provide mechanically passive energy storage and regeneration, impact mitigation, high output torque, and increased peak output power. Moreover, an SEA can provide low mechanical output impedance, good force controllability, and safety in human-machine interactions. On the other hand, the drawbacks of SEAs include low bandwidth and difficulty in controlling impulsive movements.

A QDD motor instead is simply a Geared Motor (GM) with reduced gear ratio, often limited to roughly 10:1. With QDD actuation, a low-reduction transmission results in good transparency: low backlash, back-driveability, reduced reflected inertia of the motor, and lower friction (*i.e.*, higher power transmission efficiency). Moreover, QDD actuators have high bandwidth, active compliance tuning capabilities, and good position controllability. Of course there are disadvantages in using QDD motors, such as low output torque and high Joule heating due to the necessity of working in high-current regimes.

Considering advantages and disadvantages of the two actuation mechanisms, there is a certain degree of complementarity between QDD and SEA. Recently, some researchers investigated the idea of exploiting the benefits of the these two design approaches developing a large bandwidth hybrid actuator [8], [9] that uses QDD motors and SEA in parallel, as illustrated in Fig. 1. The results are promising, but it is still unclear whether this hybrid actuation is energetically more

*This project has received funding from the Italian Ministry for Education, University, and Research (MIUR) through the "Departments of Excellence" programme.

[1]G. Grandesso, [4]M. Fontana and [5]A. Del Prete are with the Department of Industrial Engineering, University of Trento, 38123 Trento, Italy (e-mail: gianluigi.grandesso@unit.it; marco.fontana-2@unitn.it; andrea.delprete@unitn.it)

[2]G. Bravo-Palacios and [3]P. M. Wensing are with the Department of Aerospace and Mechanical Engineering, University of Notre Dame, Notre Dame, IN 46556 USA (e-mail: gbravopa@nd.edu; pwensing@nd.edu)

efficient than the single SEA or GM actuation.

In order to fairly consider the performance limitations of these systems, a framework is proposed to optimize design parameters using co-design, which simultaneously considers hardware and control in the design process. This means that hardware parameters (*e.g.*, spring stiffness, gear ratio) are included in the optimal control problem (OCP) as variables to be optimized, such that the final output is an actuation system that minimizes the energy consumed to perform a specific task. This approach, introduced for the first time in 1994 in computer graphics by Sims [10], overcomes the problems affecting the classic iterative robot design process, which relies heavily on expert knowledge, and can be highly inefficient in terms of time, cost, and final performance. The results show the value in this co-design approach, as the optimal use of the hybrid actuation is not intuitive, but can be understood from the output of the framework.

A key required aspect of the co-design framework is the definition of objectives. In a robot design process, defining goals in terms of objective functions allows for an assessment of the robot performance. This makes co-design a rigorous approach for parametric design optimization, enabling designers to obtain optimized designs tailored to perform specific tasks. A number of publications have shown the potential of co-design frameworks [11]–[16], which motivates their maturity for the case study considered here.

The contribution of this paper is a systematic design study for this hybrid actuation architecture—demonstrating how, where, and when it will provide energetic benefits over SEA or GM alone. More in details, we list here our main contributions.

- For sinusoidal motions, our analysis shows that a latching-like control strategy, similar to the one employed in energy harvesters [17], [18], is optimal using the hybrid actuation, which is able to save up to 98% of energy compared to SEA.
- For nonsinusoidal motions, we show that these large energy savings are not straightforwardly extendable. Nonetheless, the hybrid actuators can still be more energy efficient than SEA (*e.g.*, 7%), especially for proximal joints, where the weight of an actuator at the base does not contribute to the robot inertia.
- We have studied the closed-loop behavior of the hybrid actuator under perturbations. These preliminary results show that the actuation redundancy can sometimes help track the desired trajectories while maintaining low energy consumption.

II. Methods

This research starts from the analysis of the hybrid actuation applied to a 1 degree of freedom (DoF) system and then extends the study to a 2-DoF manipulator. The analysis of the 1-DoF system compares the energy consumption of this actuation, considering a DD motor instead of a QDD, with that of an SEA. In particular, considering a periodic sinusoidal motion with fixed amplitude, we investigated the variation of consumed energy as function of the oscillation frequency and other hardware parameters.

Then, we carried out the same comparative analyses of energy consumption with the 2-DoF manipulator for two specific tasks: the classic swing-up problem, and a pick-and-place operation. In addition, following a co-design approach, we included some hardware parameters as decision variables of the optimization problem. This illustrates how co-design may be a suitable way to design highly-efficient manipulators, considering both hardware and control.

A. 1-DoF: Model

As schematized in Fig. 1, the 1-DoF system with hybrid actuation consists of a link connected to the ground by a revolute joint, which is actuated simultaneously by a DD motor and an SEA. The DD acts directly on the joint, while the SEA motor is connected to it by a gearbox and a torsional spring. The link dynamics is:

$$I_l\,\ddot{\theta}(t) = \tau_s(t) - m\,g\,\cos\left(\theta(t)\right)\frac{l}{2} + \tau_{dd}(t)\,, \tag{1}$$

where $\theta(t)$ is the link angle, I_l denotes its rotational inertia around the revolute joint, m is its mass, l its length and g is gravity, while $\tau_s(t)$ and $\tau_{dd}(t)$ are respectively the output torque of the SEA spring the DD motor. The case with only SEA was considered setting $\tau_{dd}(t) = 0$.
The dynamics of the SEA motor instead is:

$$I_{se}\,\ddot{\theta}_{se}(t) = \tau_{se}(t) - \tau_r(t)\,, \tag{2}$$

where $\theta_{se}(t)$ is the SEA motor angle, $\tau_{se}(t)$ is the torque generated by the SEA motor and $\tau_r(t)$ is the load torque acting on the SEA motor. For the 1-DoF case, the spring pre-load was set to zero. The dynamics of the SEA motor is coupled with that of the link by means of the SEA gearbox and spring:

$$\tau_r(t) = \frac{1}{N\eta}K_s\left(\frac{\theta_{se}(t)}{N} - \theta(t)\right), \tag{3}$$

with K_s the SEA spring stiffness, N the gear ratio of the SEA gearbox, and η its efficiency [2], which accounts for the torque-dependent friction losses inside the gearbox. The dependency of the efficiency on the gearbox loading was neglected, as well as the fact that when the motor is not active ($\tau_{se}(t) = 0$) then the inefficiency would increase the braking capability. To further simplify the analysis in the 1-DoF case, the inertias associated with the DD motor and with the SEA gearbox were not taken into account, assuming that they are dominated respectively by the inertia of the link and that of the SEA motor. Finally, only the thermal losses of the motors were considered, neglecting Coulomb and viscous friction.

B. 1-DoF: OCP for Determining Minimal Energy Controls

The motion that was chosen for this analysis is a simple sinusoid with fixed amplitude $A = 5^\circ$ and frequency f around the vertical position of the link, *i.e.*, $\theta(t) = \pi/2 + A\sin(ft)$. Enforcing this movement, the system of equations (1)-(3)

is determined and can be solved analytically in the case with only SEA, since the only control variable is the SEA motor torque. Therefore, if a solution exists it is unique. Considering the hybrid actuation instead, the system of equations becomes under-determined because of the DD motor torque. Thus, we formulated an OCP to realize the desired motion of the link with the least amount of energy:

$$\begin{aligned} \underset{x(t),u(t)}{\text{minimize}} \quad & \Phi(x(\cdot),u(\cdot)) && \text{(4a)} \\ \text{subject to} \quad & \dot{x}(t) = f(t,x(t),u(t)) && \text{(4b)} \\ & h(t,x(t),u(t)) \leq 0 && \text{(4c)} \\ & g(t_f,x(0),x(t_f)) \leq 0 && \text{(4d)} \end{aligned}$$

The state and control trajectories, $x(t) \in \mathbb{R}^n$ and $u(t) \in \mathbb{R}^m$, are the decision variables. The objective function is represented by $\Phi(\cdot)$, while the dynamics, path and boundary constraints respectively by (4b), (4c) and (4d).
For the cost function, we chose the energy consumed to complete a cycle such that the time horizon is $t_f = 2\pi/f$. We initially neglected any capability to regenerate energy from braking:

$$\Phi(\cdot) = \int_0^{t_f} \max(0,P_{se}(t)) + \max(0,P_{dd}(t))\ dt\,, \qquad (5)$$

with P_{se} and P_{dd} the power associated respectively to the SEA and the DD motor, expressed as:

$$P_{se}(t) = \tau_{se}(t)\,\dot{\theta}_{se}(t) + \frac{\tau_{se}(t)^2}{K_m} \qquad (6)$$

$$P_{dd}(t) = \tau_{dd}(t)\,\dot{\theta}(t) + \frac{\tau_{dd}(t)^2}{K_m}\,, \qquad (7)$$

and where K_m denotes the motor constant. The introduction of the $max()$ function would cause numerical problems because of its non-differentiability at zero. To avoid this non-smooth cost, we reformulated the cost by introducing two additional variables, $\varepsilon_{se}(t)$ and $\varepsilon_{dd}(t)$:

$$\Phi(\cdot) = \int_0^{t_f} \frac{P_{se}(t)+\varepsilon_{se}(t)}{2} + \frac{P_{dd}(t)+\varepsilon_{dd}(t)}{2}\ dt \qquad (8)$$

$$\varepsilon_{se}(t) \geq -P_{se}(t), \quad \varepsilon_{se}(t) \geq P_{se}(t) \qquad (9)$$

$$\varepsilon_{dd}(t) \geq -P_{dd}(t), \quad \varepsilon_{dd}(t) \geq P_{dd}(t) \qquad (10)$$

With this formulation, when $P < 0$ the solver optimizes to $\varepsilon = -P$ so that $\frac{P+\varepsilon}{2} = 0$. When instead $P > 0$ the solver optimizes to $\varepsilon = P$ so that $\frac{P+\varepsilon}{2} = P$.

We also considered the case of energy regeneration, accounting for a battery that can be charged with 60% efficiency:

$$\begin{aligned} \Phi(\cdot) = \int_0^{t_f} \Bigg[& \frac{P_{se}(t)+\varepsilon_{se}(t)}{2} + \frac{P_{dd}(t)+\varepsilon_{dd}(t)}{2} \\ & -0.6\left(\frac{\varepsilon_{se}(t)-P_{se}(t)}{2} + \frac{\varepsilon_{dd}(t)-P_{dd}(t)}{2}\right)\Bigg]\ dt \end{aligned} \qquad (11)$$

The dynamics equations, (1)-(3), were added to the path constraints of the OCP (4), as well as the constraint to track a desired angular acceleration $\ddot{\theta}(t) + f^2 A \sin(ft) = 0$. The remaining path and boundary constraints, namely torque limits, initial and periodicity conditions, are reported in a companion technical report [19].

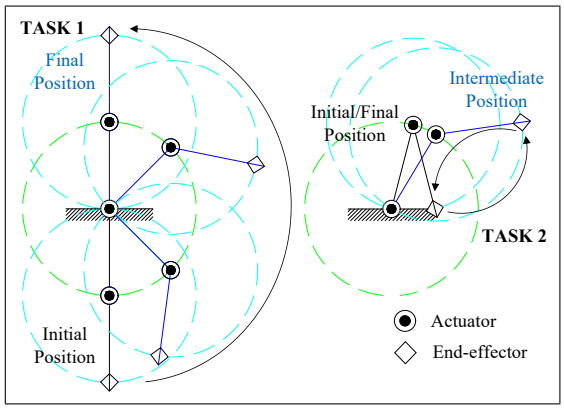

Fig. 2. Swing-up task and pick-and-place operation performed by the 2-DoF system. The green and blue circles represent instantaneous position domains for the first and second link, respectively.

C. 2-DoF: Model

The dynamics equations of the 2-DoF manipulator [20] can be found in the technical report [19]. For the 2-DoF case, we introduced a small gearbox on the DD motor because of the demanding torque requirements. Thus, what previously was called DD, is now referred to as Quasi-Direct Drive (QDD), since the gear ratio was limited to 10 [21].

D. 2-DoF: OCP for Co-Design

The energy consumption analysis begins by considering the swing-up problem, illustrated in Fig. 2. It consists of making the manipulator lift from the downward vertical configuration $(\theta_1(0) = -\pi/2,\ \theta_2(0) = 0)$ up to the upward vertical one $\left(\theta_1(t_f) = \pi/2,\ \theta_2(t_f) = 0\right)$. Thus, we formulated an OCP to minimize both the energy consumed and the time to complete this task. In an industrial context, task completion time and energy consumption both impact profits. We used weights w_1 and w_2 in the cost function to set the relative importance of these two quantities. For the sake of completeness, we first investigated the case with no energy regeneration, and then the case with it. The co-design OCP is formulated as:

$$\begin{aligned} \underset{t_f,x(t),u(t),\rho}{\text{minimize}} \quad & \Phi\left(t_f,x(t_f),u(t_f),\rho\right) && \text{(12a)} \\ \text{subject to} \quad & \dot{x}(t) = f(t,x(t),u(t),\rho) && \text{(12b)} \\ & h(t,x(t),u(t),\rho) \leq 0 && \text{(12c)} \\ & g(t_f,x(0),x(t_f/2),x(t_f),\rho) \leq 0 && \text{(12d)} \end{aligned}$$

The key aspect making this problem one of co-design is the additional decision variables in ρ, which contains the design parameters: motor masses, spring stiffnesses and gear ratios. The motor constant and inertia of each motor were related to the motor mass by the relationships presented in [15] and reported in the technical report [19]. Detailed path

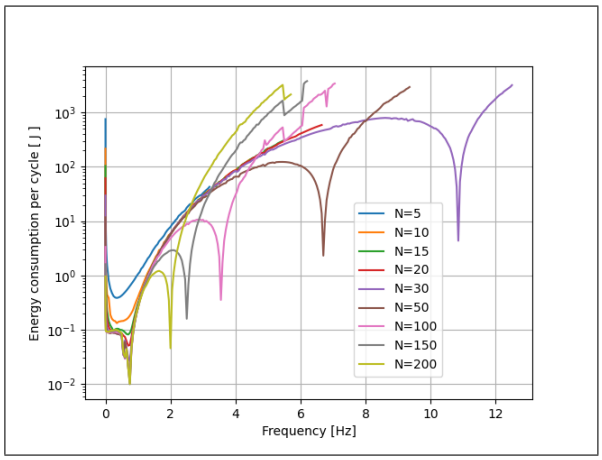

Fig. 3. Energy use as a function of the oscillation frequency for the SEA with spring constant $K_s = 30\,\mathrm{Nm/rad}$ and 9 different gear ratios N.

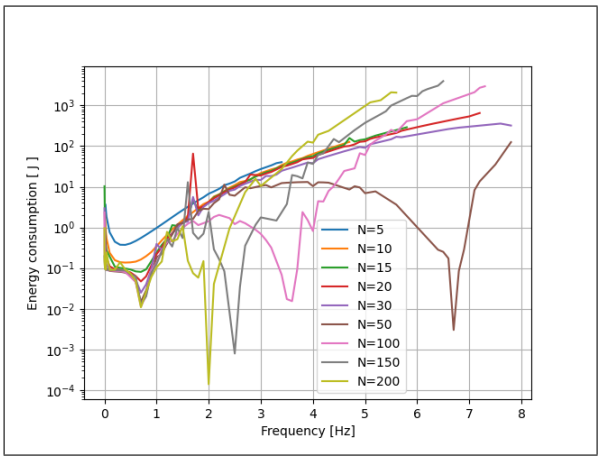

Fig. 4. Energy use as a function of the oscillation frequency for the hybrid actuator with spring constant $K_s =$ Nm/rad and 9 different gear ratios N.

and boundary constraints (12c) and (12d) are provided in [19] as well.

Without energy regeneration, the expression of the cost function (12a) is:

$$\Phi(\cdot) = w_1 \int_0^{t_f} \left(\sum_{k=1}^{2} \frac{P_{se,k}(t,\rho) + \varepsilon_{se,k}(t,\rho)}{2} + \right. \\ \left. + \sum_{k=1}^{2} \frac{P_{dd,k}(t,\rho) + \varepsilon_{dd,k}(t,\rho)}{2} \, dt \right) + w_2 t_f^2 \tag{13}$$

To avoid trivial solutions that would have exploited only the torque given by the pre-load of the SEAs springs, for this task we set the pre-load to zero.

The effects of this hybrid actuation were also studied considering a pick-and-place operation for a 2-DoF manipulator (see Fig. 2). The task consists in moving the manipulator from an initial configuration to a certain position of the end-effector, and then bringing it back to the initial configuration. Specifically, the initial/final configuration is given by the end-effector being at the same height of the first joint and at a distance of $l_1/2$ from it, while in the intermediate configuration the end-effector reaches a height of l_1 and a distance of $3l_1/2$.

For this task, we let the springs pre-load free, however adding as constraint that the final pre-load must be equal to the initial one.

III. Results

This section reports the results for the 1-DoF and 2-DoF models. First, we compare the energy consumption of the hybrid actuator and SEA for the 1-DoF system. We found that for sinusoidal motions the energy saving using the hybrid actuation can exceed 90%. Moreover, the optimal control strategy is very similar to the latching control used in energy harvesters [17], [18].

With the 2-DoF system, the comparison extends also to GMs (*i.e.*, DC motors attached to gearboxes with gear ratios up to $N = 200$), hybrid actuation at both the joints, and hybrid actuation at the first joint and SEA at the second joint. The 2-DoF system carried out two different tasks: swing-up and pick-and-place. A co-design framework was built to find optimal hardware parameters and control trajectories for each task. Our analysis shows that, even though latching-like control is not optimal for nonsinusoidal motions, the hybrid actuation is still more efficient than SEAs and GMs.

In addition, we studied also the closed-loop behavior of the actuators under perturbations. Even though these last results are preliminary, we found that tracking the desired trajectories while maintaining low energy consumption can sometimes be facilitated by the hybrid actuator redundancy.

A. 1-DoF: Test Details

The test with the 1-DoF system consists of fixing the motion of the joint (sinusoid) and optimizing the hybrid actuation control to minimize the energy consumption. In the case with only the SEA, the motor torque is analytically determined. The frequency range in the analysis goes from 0.1 to 10 Hz, with 0.1 Hz resolution. The set of values for the spring stiffness is $[30, 50, 100]\,\mathrm{Nm/rad}$, while for the gear ratio of the SEA it is $[5, 10, 15, 20, 30, 50, 100, 150, 200]$.

The same brushless DC motor model was considered for both the SEA and the DD motor. Motor specifications include: peak torque $\tau_{max} = 7.13\,\mathrm{Nm}$, rotor inertia $I_{se} = 10^{-5}\,\mathrm{kgm^2}$ and motor constant $K_m = 0.64\,\mathrm{Nm}/\sqrt{\mathrm{Watt}}$. The gearbox efficiency was considered to scale exponentially with the gear ratio as suggested in [15].

For all the possible combinations of oscillation frequency, spring stiffness and gear ratio, the OCP (4) was specified using the optimization modeling language PYOMO [22], [23] and solved using IPOPT [24] with the MA57 linear solver [25]. The OCP was transcribed using direct collocation with a Lagrange-Radau scheme, 30 finite elements, and 3 collocation points per element.

B. 1-DoF: Test Results

Our results show that the hybrid actuation is energetically more efficient than the SEA. Fig. 3 shows the energy consumption of the SEA, considering a 30 Nm/rad spring

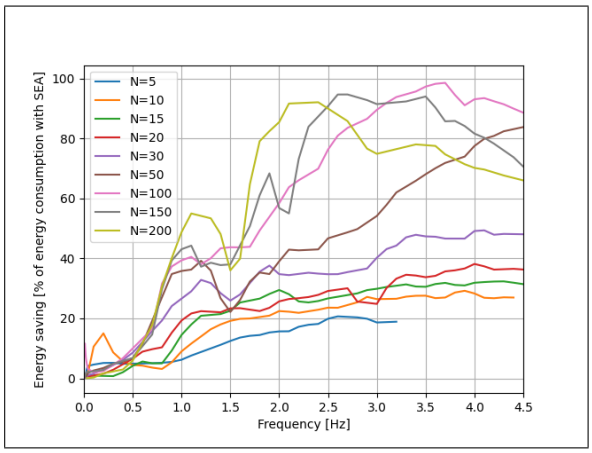

Fig. 5. Energy saving of the hybrid actuation expressed as percentage of SEA energy consumption.

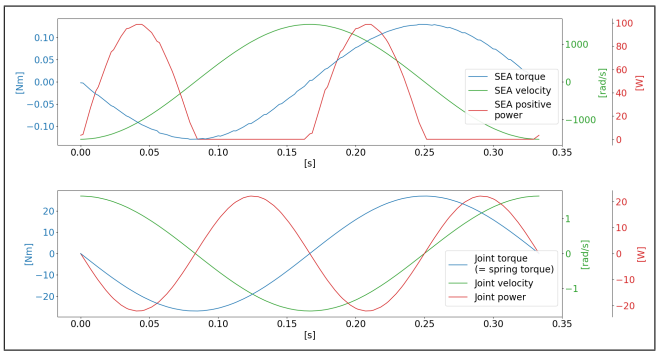

Fig. 6. SEA: torque, velocity and power of motor and joint required to perform a 3Hz sinusoidal motion. The SEA positive power is the maximum between zero and the power consumed by the SEA (no energy regeneration case).

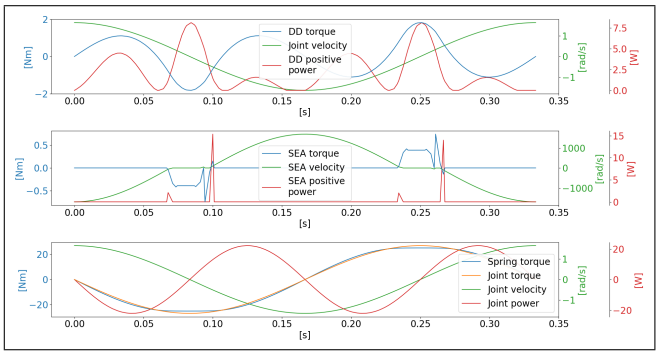

Fig. 7. Hybrid actuation: torque, velocity and power of motors and joint required to perform a 3Hz sinusoidal motion. The DD and SEA positive power is the maximum between zero and the power consumed respectively by the DD and the SEA (no energy regeneration case).

stiffness and different gear ratios, while Fig. 4 shows the case with hybrid actuation. Both cases assumed no energy regeneration. The valleys in Fig. 3 occur at the system natural frequencies, which vary depending on the gear ratio. Indeed, the higher the gear ratio, the lower the system natural frequency. The natural frequency also depends also on the spring stiffness: fixing the gear ratio, the natural frequency shifts to higher values as the spring stiffness increases.

To better understand the energy advantage of the hybrid actuation, Fig. 5 illustrates the energy savings achieved with the hybrid actuation as a percentage of the SEA energy consumption. To improve readability, we filtered the data of Fig. 5 with an analog Butterworth filter of order 1 with critical frequency equal to $0.2\,\mathrm{rad/s}$. The energy savings can be extremely large, up to 98%, depending on the oscillation frequency, the gear ratio and the spring stiffness. For instance, in the range 3-4 Hz with $N = 100$ and $K_s = 30\,\mathrm{Nm/rad}$, the hybrid actuation can save up to 90% of energy compared to the SEA. On the other hand, at 1 Hz the energy saving is much lower: about 40% for high gear ratios ($N \geq 100$), and less than 20% for low gear ratios ($N \leq 20$).

Insight into the large energy savings achievable with the hybrid actuation comes from how each actuator produces the desired joint torque. With only the SEA, the torque is provided only by the spring, while with the hybrid actuation it comes also from the DD motor. The spring torque mainly stems from the motion of the SEA rotor being opposite to that of the joint. Since in this test the joint trajectory is fixed, the SEA rotor angle completely defines the spring torque. Thus, with only the SEA, the analytical solution for the rotor angle trajectory can be computed. To make the rotor achieve this motion, the motor must provide a sinusoidal torque (opposite to the spring torque which is seen as load torque by the SEA). For instance, Fig. 6 compares the torque, angular velocity, and power from the SEA and the load for $N = 100$, $Ks = 30\,\mathrm{Nm/rad}$ and $f = 3\,\mathrm{Hz}$, which led to more than 90% of energy saving. As the figure shows, the SEA motor must be always powered, which implies a high energy consumption due to the SEA motor velocity reaching very high values (up to $1500\,\mathrm{rad/s}$). In two large time intervals the SEA positive power (due to no energy regeneration) is greater than zero and reaches almost 100 W.

With the hybrid actuation instead, the SEA motor is powered only during two short intervals ($0.07 - 0.1\,\mathrm{s}$ and $0.22 - 0.26\,\mathrm{s}$), when it almost halts the motion of its rotor (see Fig. 7). The SEA rotor is not completely blocked so that the thermally dissipated power is compensated by negative mechanical power, resulting in nearly always nonpositive total power. It is interesting to notice that the solver found a control strategy very similar to the *latching control*, which is implemented in many energy harvesters to maximize energy generation, by keeping the SEA rotor velocity in counter-phase with the joint velocity [17], [18]. This strategy is applicable thanks to the DD motor, which provides the additional torque needed to perform correctly the sinusoidal motion. Since this torque is rather small, as well as the joint velocity, the overall energy consumption remains small (peak positive power less than 8 W).

C. 2-DoF: Test Details

We considered four actuation architectures: only GMs, only SEAs, hybrid actuation on both joints (Full Hybrid) and hybrid actuation on the first joint with SEA on the second one (Hybrid+SEA). For both tasks, we set the weights $w_1 = 1$ (associated to energy) and $w_2 = 0.1$ (associated to time) in

TABLE I

TASK COMPLETION TIME AND ENERGY CONSUMPTION WITH DIFFERENT ACTUATION ARCHITECTURES.

Architecture	Task Time [s]		Energy [J]		Cost function	
	Swing Up	*Pick&Place*	*Swing Up*	*Pick&Place*	*Swing Up*	*Pick&Place*
GMs	5.71	3.38	226.68	42.57	229.94	43.72
SEAs	4.17	1.36	225.17	0.86	226.90	1.04
Full Hybrid	10.89	1.59	264.72	1.16	276.59	1.42
Hybrid + SEA	5.25	1.37	214.01	0.80	216.77	0.99

the cost function (13). Moreover, to improve accuracy, we increased the number of finite elements to 100. Finally, we also investigated the case with 60% energy regeneration.

Since the solution that IPOPT could find was strongly biased by the initialization values of the hardware design parameters, it was necessary to randomize the initialization values and repeat the simulations 40 times. Beyond 40 random initial guesses, the change in the best solution was found to be negligible.

D. 2-DoF: Test Results

1) Swing-Up: The following results concern a swing-up task with no load. Tab. I summarizes the results with no energy regeneration, and compares the energy consumption and task completion time of the different actuation architectures. The Full Hybrid actuation turned out to be the least effective, in terms of both energy consumption and task completion time. Instead, the Hybrid+SEA configuration performed the best. It allowed for a 5% energy saving compared to only SEAs, with a 26% increase in task completion time. In contrast, when compared to only GMs, around the same energy saving comes accompanied by an 8% reduction in completion time. Tab. I reports also the objective function values, supporting the fact that the Hybrid+SEA configuration is the best choice for the swing-up problem.

Table II lists the optimal hardware parameters found from solution of the OCP (12a) using a co-design framework. In all cases, the mass of the motors on the first joint is equal to its upper bound (10 kg), while for the motors on the second joint the optimal mass corresponds to the lower bound (0.1 kg). This is reasonable: the inertia seen at the first joint would increase if the motors on the second joint were heavier, while the motors actuating the first joint are located at the robot base and thus do not increase the inertia. The optimal gear ratios on the second joint in both cases with GMs and with Full Hybrid actuation are at the lower bound, namely 1. Therefore, the GM and QDD at the second joint contribute very little to the motion, while considerably increasing the inertia of the system; for this reason the solver sets also the motor masses to the lower bound.

This finding motivated us to investigate the design with hybrid actuation at the first joint and only SEA at the second one. That the optimal gear ratios of the SEAs on the second joint are at their upper bound means that the solver tries to maximize the contribution of these SEAs without increasing the inertia of the system. However, if the gearbox mass was modelled as function of the gear ratio, then the optimal gear ratios would be lower than 200 because they would affect directly the system inertia and so the energy use.

2) Pick and Place: Table III summarizes the results of the pick-and-place operation. The three actuation systems that employ SEAs clearly outperform the one with GMs. This is due to the task periodicity, which allows to exploit the springs pre-load to perform the motion. As observed with the swing-up task, also in this case the best results are achieved using the hybrid actuation on the first joint and SEA on the second one. Compared to the Full Hybrid actuation, the energy savings is 31% and the completion time is reduced by 13.8%. Considering the case with only SEAs instead, the task can be performed taking almost the same time but consuming 7% less energy.

As observed with the swing-up task, in all cases the optimal mass of the motors on the first joint is the maximum allowed, as it happens also for the gear ratios of the SEAs on the second joint, while the optimal motor mass of the QDD on the second joint of the Full Hybrid actuation as

TABLE II

CO-DESIGN RESULTS FOR SWING-UP TASK.

Architecture	Motor Mass [kg]		Gear Ratio		Spring Stiffness
	GM	*QDD*	*GM*	*QDD*	*[N·m/rad]*
1^{st} GM	10.00	—	18.79	—	—
2^{nd} GM	0.10	—	1.00	—	—
1^{st} SEA	10.00	—	21.25	—	139.12
2^{nd} SEA	0.10	—	200.00	—	17.21
1^{st} Hybrid	10.00	10.00	8.51	8.47	43.61
2^{nd} Hybrid	0.10	0.10	200.00	1.00	74.88
1^{st} Hybrid	10.00	0.10	13.35	10.00	70.65
2^{nd} SEA	0.10	—	200.00	—	24.75

TABLE III

CO-DESIGN RESULTS FOR PICK&PLACE TASK.

Architecture	Motor Mass [kg]		Gear Ratio		Spring Stiffness
	GM	*QDD*	*GM*	*QDD*	*[N·m/rad]*
1^{st} GM	10.00	—	89.41	—	—
2^{nd} GM	4.34	—	10.71	—	—
1^{st} SEA	10.00	—	200.00	—	250.00
2^{nd} SEA	3.17	—	200.00	—	9.23
1^{st} Hybrid	10.00	10.00	200.00	5.66	250.00
2^{nd} Hybrid	2.75	0.10	200.0	1.00	5.51
1^{st} Hybrid	10.00	10.00	200.00	4.52	250.00
2^{nd} SEA	3.18	—	200.00	—	9.18

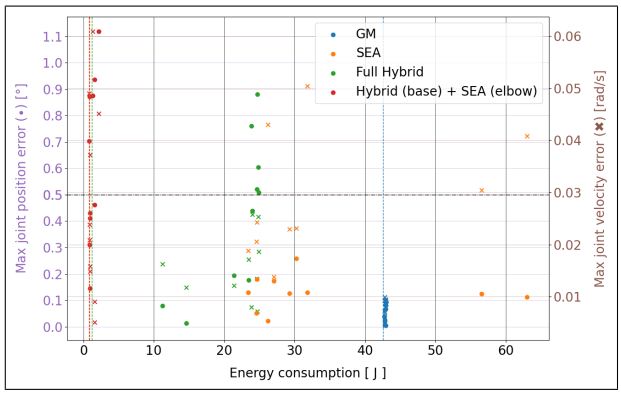

Fig. 8. Pick-and-Place Task: energy consumption and maximum final joint-state error with PD control and disturbances in the optimized hardware parameters as well as impulsive variations of joint accelerations.

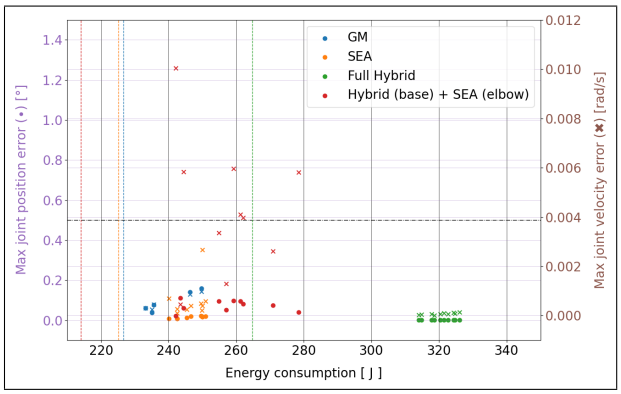

Fig. 9. Swing-Up Task: energy consumption and maximum intermediate and final joint-state error with PD control and disturbances in the optimized hardware parameters as well as impulsive variations of joint accelerations.

well as its gear ratio hit the lower bounds. The fact that the values of gear ratio of the SEAs on the first joint are equal to their upper bound may be due to the high-torque demanding static conditions set for this task in the initial-intermediate-final configurations. With this task, it is not convenient to adopt the strategy of using the SEAs to store and release mechanical power through the swinging motion of the links, as in the case of the swing-up task. This may explain why the solver sets the spring stiffnesses of the SEAs on the first joint to the maximum value, so as to increase the bandwidth of the SEAs.

The results up to this point suggest that a periodic task can be efficiently achieved in ideal settings using SEAs, thanks to their capability to store and release mechanical power without wasting energy. The benefits of adding a DD in parallel to the SEA in the 1-DoF system, that allows for a latching control strategy, were observed only to a small extent with the 2-Dof system and the tasks considered. Nonetheless, choosing other tasks may highlight more effectively the energy efficiency of the hybrid actuation.

E. 2-DoF: Feedback Control

The previous subsections investigated the energy efficiency of different actuation architectures (SEA, GM, Full Hybrid, Hybrid+SEA) in ideal settings, showing that the hybrid actuator and Hybrid+SEA can lead to energy savings. However, this does not suffice to claim that this actuator could perform well in the real world. For this reason, we now analyse how different actuators behave in more realistic settings, in which the system has to cope with modeling errors and disturbances using feedback control.

To this end, we used a PD controller with hand-tuned gains to observe how energy consumption and task completion accuracy varied due to modeling errors in the hardware parameters and joint acceleration disturbances. We carried out 10 simulations for each actuation system, randomly selecting the magnitude of the disturbances up to 1% of the nominal value of the optimized hardware parameters and considering impulsive variations of the joint accelerations ($10\,\mathrm{rad/s^2}$) randomly occurring between 25% and 75% of the task completion time. Figs. 8 and 9 show the energy consumption and the maximum joint state error for the pick-and-place operation and swing-up task, respectively. The error is measured at the intermediate and final state for the pick-and-place task and only at the final state for the swing-up task. The dashed vertical lines represent the energy consumption in absence of any disturbance, while the dashed horizontal line is a subjective threshold representing the maximum position error (0.5°) below which we consider the task successful. Since nominal energy consumption with only SEAs and with Hybrid+SEA are very similar (respectively 0.86 J and 0.80 J), the corresponding lines overlap.

In the pick-and-place task, the open-loop behavior of the system with Hybrid+SEA also extends to closed-loop with disturbances: the energy consumption is very close to the nominal one, although the maximum joint position error exceeds the threshold in half of the simulations. The GM actuation also ensures an energy consumption very close to the nominal one, in addition to an overall high accuracy and precision. The other two actuation systems instead perform poorly both in terms of actual energy consumption and task accuracy. Overall, the maximum position and velocity errors considering the intermediate and final configurations remain consistently bounded.

The results are different for the swing-up task: SEA and Hybrid+SEA perform similarly, while good accuracy is obtained with Full Hybrid actuation to the detriment of a high increment in energy consumption. In Fig. 9, the results of only 5 simulations with GMs are shown because in half of the simulations the controller failed to stabilize the system. In terms of accuracy compared to the pick-and-place task, the results for the swing-up task may be explained by the instability of the desired final configuration. An exception is represented by the Full Hybrid actuation, which may benefit from the combined action of QDD and SEA on the second joint to better reject acceleration disturbances.

IV. Conclusions

This study presented an energy efficiency analysis of a hybrid actuation system based on a co-design framework. The analysis starts from a simple case study, which examines the energy consumption of an oscillating 1-DoF system. A

frequency study was carried out to investigate the behavior of the hybrid actuation compared to a SEA in terms of energy consumption. Then we focused on a 2-DoF planar manipulator. We considered two tasks and used co-design to make optimal choices in the simultaneous design of hardware and control. Finally, we investigated the closed-loop behavior of the different actuation systems subject to modeling errors and disturbances using PD control to track the previously computed optimal trajectories.

The results show that the proposed hybrid actuation is energetically convenient compared to standard actuators as SEAs or GMs. With the 1-DoF system performing a sinusoidal motion, the energy savings compared to an SEA can be very large, sometimes exceeding 90%. For the 2-DoF system instead, the energy savings turns out to be task dependent, but in any case the best configuration consists of having hybrid actuation on the first joint and an SEA on the second one. This system can outperform GMs (up to 98% energy consumption reduction), but it leads to limited savings (up to 7%) with respect to only SEAs. This finding suggests that transmission designs (e.g, as in [26]) relating sinusoidal angle/torque input trajectory of the actuator to nonsinusoidal output trajectories might be pursued to enable significant energy savings for other behaviors. In addition, for a pick-and-place task, the energetic advantages of the hybrid actuation also extend to closed-loop control with perturbations. With the proposed co-design framework, it was possible not only to study and verify the energy convenience of this hybrid actuation, but also to obtain optimal values for its hardware parameters and optimal state-control trajectories. Furthermore, co-design shows that there is increased incentive for adopting hybrid actuation for more proximally located joints. This suggests that the importance of designing transmission systems to relay power distally will be even more important for designs adopting hybrid actuation schemes.

To improve the analysis of closed-loop energy efficiency for different actuation systems, future work will explore the possibility of computing optimal feedback gains using parametric optimization. Another future development will be the extension of this study to a single leg of a quadruped subject to different gaits, obtaining optimal hardware designs and control trajectories via simulation, and analyzing the energy efficiency of diverse actuation configurations in a real application. Finally, a mixed-integer OCP could be formulated to let the solver choose which actuation system is the best to actuate each single joint.

REFERENCES

[1] G. A. Pratt and M. M. Williamson, "Series elastic actuators," in *Proc. IEEE International Conference on Intelligent Robots and Systems (IROS)*, Pittsburgh, Pennsylvania, Aug. 1995, pp. 399–406.

[2] C. Lee, S. Kwak, J. Kwak, and S. Oh, "Generalization of series elastic actuator configurations and dynamic behavior comparison," *Actuators*, vol. 6, pp. 1–26, Aug. 2017.

[3] S. Seok, A. Wang, D. Otten, and S. Kim, "Actuator design for high force proprioceptive control in fast legged locomotion," in *Proc. IEEE International Conference on Intelligent Robots and Systems (IROS)*, Vilamoura, Portugal, Dec. 2012, pp. 1970–1975.

[4] P. M. Wensing, A. Wang, S. Seok, D. Otten, J. Lang, and S. Kim, "Proprioceptive actuator design in the mit cheetah: Impact mitigation and high-bandwidth physical interaction for dynamic legged robots," *IEEE T. Robot.*, vol. 33, pp. 509–522, Sept. 2017.

[5] G. Kenneally, A. De, and D. E. Koditschek, "Design principles for a family of direct-drive legged robots," *IEEE Robot. Autom. Lett.*, vol. 1, pp. 900–907, July 2016.

[6] A. G. Leal Junior, R. M. de Andrade, and A. B. Filho, "Series elastic actuator: Design, analysis and comparison," *Recent Advances in Robotic Systems*, Sept. 2016.

[7] K. Y. T. H. Asada, *Direct-Drive Robots, Theory and Practice*. Cambridge, Massachusetts: MIT Press, 1987.

[8] J. B. Morrell and J. K. Salisbury, "Parallel-coupled micro-macro actuators," *Int. J. Robot. Res.*, vol. 17, pp. 773–791, July 1998.

[9] M. Zinn, B. Roth, O. Khatib, and J. K. Salisbury, "A new actuation approach for human friendly robot design," *Int. J. Robot. Res.*, vol. 23, pp. 379–398, Apr. 2004.

[10] K. Sims, "Evolving virtual creatures," in *Proc. 21st annual conference on Computer graphics and interactive techniques (SIGGRAPH)*, Orlando, Florida, July 1994, pp. 15–22.

[11] N. Cheney, R. MacCurdy, J. Clune, and H. Lipson, "Unshackling evolution: Evolving soft robots with multiple materials and a powerful generative encoding," in *Proc. 15th Annual Conference on Genetic and Evolutionary Computation (GECCO)*, Amsterdam, Netherlands, July 2013, p. 167.

[12] K. M. Digumarti, C. Gehring, S. Coros, J. Hwangbo, and R. Siegwart, "Concurrent optimization of mechanical design and locomotion control of a legged robot," in *Proc. 17th International Conference on Climbing and Walking Robots (CLAWAR)*, Poznań, Poland, July 2014, pp. 315–323.

[13] J. Hass, J. M. Herrmann, and T. Geisel, "Optimal mass distribution for passivity-based bipedal robots," *Int. J. Robot Res.*, vol. 25, pp. 1087–1098, Nov. 2006.

[14] Q. Li, W. J. Zhang, and L. Chen, "Design for control-a concurrent engineering approach for mechatronic systems design," *IEEE ASME Trans. Mechatron.*, vol. 6, pp. 161–169, June 2001.

[15] Y. Yesilevskiy, Z. Gan, and C. Remy, "Energy-optimal hopping in parallel and series elastic 1d monopeds," *J. Mech. Robot.*, vol. 10, Mar. 2018.

[16] G. Bravo-Palacios, A. Del Prete, and P. M. Wensing, "One robot for many tasks: Versatile co-design through stochastic programming," *IEEE RA-L*, vol. 5, no. 2, pp. 1680–1687, Apr. 2020.

[17] A. Babarit and A. H. Clement, "Optimal latching control of a wave energy device in regular and irregular waves," *Appl. Ocean Res.*, vol. 28, pp. 77–91, Apr. 2006.

[18] F. Saupe, J. C. Gilloteaux, P. Bozonnet, Y. Creff, and P. Tona, "Latching control strategies for a heaving buoy wave energy generator in a random sea," in *19th IFAC*, Cape Town, South Africa, Aug. 2014, pp. 7710–7716.

[19] G. Grandesso, G. Bravo-Palacios, P. M. Wensing, M. Fontana, and A. Del Prete, "Exploring the limits of a hybrid actuation system through co-design - technical report," University of Trento, Tech. Rep., 2020. [Online]. Available: https://hal.archives-ouvertes.fr/hal-02737086

[20] M. W. Spong, "The swing up control problem for the acrobot," *IEEE Control Syst. Mag.*, vol. 15, pp. 49–55, Feb. 1995.

[21] N. Kau, A. Schultz, N. Ferrante, and P. Slade, "Stanford doggo: An open-source, quasi-direct-drive quadruped," in *Proc. IEEE International Conference on Robotics and Automation (ICRA)*, Montreal, Canada, May 2019, pp. 6309–6315.

[22] W. E. Hart, J. Watson, and D. L. Woodruff, "Pyomo: modeling and solving mathematical programs in python," *Math. Prog. Comp.*, vol. 3, pp. 219–260, Aug. 2011.

[23] W. E. Hart, C. Laird, J. Watson, D. L. Woodruff, G. A. Hackebeil, B. L. Nicholson, and J. D. Siirola, *Pyomo — Optimization Modeling in Python*, 2nd ed. Springer International Publishing, 2017.

[24] A. Wächter and L. T. Biegler, "On the implementation of a primal-dual interior point filter line search algorithm for large-scale nonlinear programming," *Math. Program.*, vol. 106, pp. 25–57, Mar. 2006.

[25] (2013) Hsl: A collection of fortran codes for large scale scientific computation. [Online]. Available: http://www.hsl.rl.ac.uk

[26] S. Coros, B. Thomaszewski, G. Noris, S. Sueda, M. Forberg, R. W. Sumner, W. Matusik, and B. Bickel, "Computational design of mechanical characters," *ACM Transactions on Graphics (TOG)*, vol. 32, no. 4, pp. 1–12, 2013.